J. Fluid Mech. (2004), *vol.* 498, *pp.* 315–332.
DOI: 10.1017/S0022112003006797 Printed in the United Kingdom

Reynolds number dependence of an upper bound for the long-time-averaged buoyancy flux in plane stratified Couette flow

By C. P. CAULFIELD[1], W. TANG[1] AND S. C. PLASTING[2]

[1]Department of Mechanical and Aerospace Engineering, Jacobs School of Engineering, University of California, San Diego, 9500 Gilman Drive, La Jolla, CA 92093-0411, USA

[2]School of Mathematics, University of Bristol, University Walk, Bristol BS8 1TW, UK

(Received 21 April 2003 and in revised form 20 August 2003)

We derive an improved rigorous upper bound for the long-time-averaged vertical buoyancy flux for stably stratified Couette flow; i.e. the flow of a Boussinesq fluid (with reference density ρ_0, kinematic viscosity ν, and thermal diffusivity κ) confined between two parallel horizontal plates separated by a distance d, which are driven at a constant relative velocity ΔU, and are maintained at a constant (statically stable) temperature difference leading to a constant density difference $\Delta\rho$. We construct the bound by means of a numerical solution to the 'background method' variation problem as formulated by Constantin and Doering using a one-dimensional uni-directional background. The upper bound so constructed is the best possible bound with the imposed constraints for streamwise independent mean flows that are statistically steady, and is calculated up to asymptotically large Reynolds numbers. We find that the associated (dimensional) upper bound $\mathscr{B}^*_{max}$ on the long-time-averaged and volume averaged buoyancy flux $\mathscr{B}^* := \lim_{t\to\infty}(1/t)\int_0^t \langle \rho u_3\rangle g/\rho_0 \,\mathrm{d}\tilde{t}$ (where u_3 is the vertical velocity, g is the acceleration due to gravity, and angled brackets denote volume averaging) does not depend on either the bulk Richardson number $J = g\Delta\rho d/(\rho_0\Delta U^2)$ of the flow, or the Prandtl number $\sigma = \nu/\kappa$ of the fluid. We show that $\mathscr{B}^*_{max}$ has the same inertial characteristic scaling as the (dimensional) mechanical energy dissipation rate $\mathscr{E}^*_B$, and $\mathscr{B}^*_{max} = 0.001267\Delta U^3/d$ as $Re\to\infty$. The associated flow structure exhibits velocity boundary layers embedded within density boundary layers, with local gradient Richardson numbers $Ri = O(\sigma/Re) \ll 1$ in the vicinity of the horizontal plates. There is a correspondence between the predicted flow structure and the flow structure at a lower Reynolds number associated with the upper bound on the mechanical energy dissipation rate $\mathscr{E}^*_{max}$ in an unstratified fluid. We establish that, for the flow that maximizes the buoyancy flux, the flux Richardson number $Ri_f \to 1/3$ as $Re\to\infty$, independently to leading order of both Re and J. There is a generic partition of the energy input by the shear into the fluid into three equal parts: viscous dissipation of kinetic energy by the mean flow; viscous dissipation of kinetic energy by perturbation velocities; and vertical buoyancy flux.

1. Introduction

Flows where both the mean horizontal velocity and mean density distributions vary with height (i.e. stably stratified shear flows) are ubiquitous in the environment.

An important question is how such turbulent, inherently small-scale motions cause 'mixing', and so irreversibly modify the density distribution. Such irreversible mixing processes lead to transport of heat and/or salinity within the atmosphere or ocean. There has been a wide range of research trying to gain a detailed understanding of mixing within stratified shear flows in general (see, for example, Fernando 1991; Peltier & Caulfield 2003). It would clearly be useful if constraints or bounds could be found for the rate of mixing, (or equivalently the long-time-averaged buoyancy flux) within stratified shear flows, and that is the principal objective of the work which we report here.

It is not only the total amount of mixing that is of significant practical interest, but also its 'efficiency', in the sense of the proportion of the work done on a stratified fluid that leads to irreversible mixing, as opposed to being 'lost' to viscous dissipation. This ratio is often referred to as the flux Richardson number Ri_f (see Turner 1973; Linden 1979; Fernando 1991) and its parameterization is very important to larger scale models of, for example, ocean circulation. The dimensional volume and long-time-averaged buoyancy flux $\mathscr{B}^*$ is defined as

$$\mathscr{B}^* := \lim_{t\to\infty} \frac{1}{t} \int_0^t \frac{g}{\rho_0} \langle \rho u_3 \rangle \, \mathrm{d}\tilde{t}, \tag{1.1}$$

where g is the acceleration due to gravity, ρ_0 is a reference density, angled brackets denote an appropriate volume average, and u_3 is the vertical flow velocity, while the long-time-averaged (dimensional) mechanical energy dissipation $\mathscr{E}^*$ is defined as

$$\mathscr{E}^* := \lim_{t\to\infty} \frac{1}{t} \int_0^t \nu \langle \|\nabla \boldsymbol{u}\|^2 \rangle \, \mathrm{d}\tilde{t} = \lim_{t\to\infty} \frac{1}{t} \int_0^t \nu \langle |\nabla u_1|^2 + |\nabla u_2|^2 + |\nabla u_3|^2 \rangle \, \mathrm{d}\tilde{t}. \tag{1.2}$$

Using this notation, an appropriate definition for the flux Richardson number Ri_f is then

$$Ri_f = \frac{\mathscr{B}^*}{\mathscr{B}^* + \mathscr{E}^*}. \tag{1.3}$$

Much evidence and modelling (see e.g. Linden 1979; Osborn 1980; Fernando 1991; Gargett & Moum 1995; Moum 1996; Ruddick, Walsh & Oakey 1997; Caulfield & Peltier 2000; Smyth, Moum & Caldwell 2001) point to a typical value of this parameter being $Ri_f \sim 0.15 - 0.25$. However, recent observations and measurements (Strang & Fernando 2001; Pardyjak, Monti, & Fernando 2002) suggest that substantially larger values $Ri_f \sim 0.3 - 0.45$ are possible. Various semi-empirical scaling arguments have been presented to construct heuristic bounds on mixing (Townsend 1958; Monin & Yaglom 1971; Turner 1973).

However, a method (as originally proposed by Malkus 1954, 1956; and substantially developed by Howard 1963, 1972, 1990; Busse 1969*a*, *b*, 1970, 1978) has also been constructed to generate rigorous bounds on important flow quantities (see Busse 1978 for a review). Perhaps because of the complexity of the required analysis, the predictions of the Howard–Busse method were not as widely tested as might be expected until the recent development of an alternative variational technique, the so-called 'background method' due to Doering and Constantin (see Doering & Constantin 1992, 1994, 1996; Constantin & Doering 1995; Gebhardt *et al.* 1995; Nicodemus, Grossman & Holthaus 1997*a*, *b*, 1998*a*, *b*). This method critically relies on an insight due to Hopf (1941), and so, following Plasting & Kerswell (2003, hereinafter referred to as PK03) it seems appropriate to refer to the method as the CDH method.

The CDH method, which will be the focus of this paper, uses a non-unique decomposition of both the velocity and density distributions into a steady 'background' that satisfies the actual inhomogeneous boundary conditions of the flow, and a 'fluctuation' away from this background with homogeneous boundary conditions. Such decompositions can then be used to construct rigorous upper bounds on flow quantities of interest, consistently with imposed dynamic and kinematic constraints. As established in a sequence of important papers by Kerswell (1997, 1998, 2001), the CDH method produces a complementary variational problem to that constructed by the Howard–Busse method.

A particularly attractive class of possible background fields that has some of the physical structure that is expected as Reynolds number increases, and also allows significant analytical progress, is the class of piecewise linear background flow fields (Doering & Constantin 1992). This class was also used to construct analytically a rigorous bound for the long-time-averaged buoyancy flux within stratified plane Couette flow by Caulfield & Kerswell (2001, hereinafter referred to as CK01). We generalize their results in this paper. The bound in CK01 was constructed conservatively by restricting attention to fluctuations with non-zero horizontal mean components only. In other words, the only non-zero differences allowed between the total velocity and density fields and the chosen 'background' velocity and density fields) were differences in the horizontal mean components.

Under these assumptions, CK01 found that the dimensional volume and long-time-averaged buoyancy flux $\mathscr{B}^*$, defined in (1.1), had a rigorous upper bound

$$\mathscr{B}^* \leqslant \mathscr{B}^*_{max} = \frac{\Delta U^3}{64\sqrt{2}d}\left(1 - \frac{16\sqrt{2}}{Re}\right) = 0.01105\frac{\Delta U^3}{d} - 0.25\frac{\Delta U^2 \nu}{d^2}, \tag{1.4}$$

with associated long-time-averaged dimensional mechanical energy dissipation rate $\mathscr{E}^*$ (as defined in (1.2)) given by

$$\mathscr{E}^* = \frac{\Delta U^3}{64\sqrt{2}d}\left(1 + \frac{48\sqrt{2}}{Re}\right) = 0.01105\frac{\Delta U^3}{d} + 0.75\frac{\Delta U^2 \nu}{d^2}. \tag{1.5}$$

In the limit as $Re \to \infty$, this particular restrictive bound is independent of both the overall stratification of the system, and the diffusivities of momentum and density within the fluid. Also, to leading order there is an equipartition between the energy lost from the driving shear due to the buoyancy flux, and the energy lost due to viscous dissipation, which, owing to the assumption that the fluctuation fields have no meanless parts, corresponds to the viscous dissipation associated with the horizontally averaged flow velocity. This equipartition implied that the efficiency of the mixing (or, equivalently, the flux Richardson number Ri_f, defined in (1.3)) approached 1/2 as $Re \to \infty$.

Recently, the fundamental issue of relaxing the assumption of particular trial functions in the determination of bounds was addressed by PK03, for the canonical problem of generating a rigorous upper bound on the mechanical energy dissipation rate in (unstratified) plane Couette flow. They formulated the complete CDH method variational problem for one-dimensional uni-directional background velocity fields, subject to the dynamical constraints of total power balance, and horizontally averaged along stream momentum balance. They then solved the problem numerically using the continuation program PITCON (Rheinboldt & Burkhardt 1983*a*, *b*) to asymptotically large Reynolds numbers. They found that, as $Re \to \infty$, the dimensional upper bound on the mechanical energy dissipation rate $\mathscr{E}^*_{max} \to 0.008553\Delta U^3/d$, a 21%

improvement on the best value of Nicodemus *et al.* (1998*b*) and consistent with the bounds determined by Busse (1970) when appropriate error estimates (Busse 1968) are included. The numerical calculations of PK03 also demonstrated that the multiple boundary-layer Howard–Busse method captured the main features of the best possible bounding structure, showing that an increasing number of nested boundary layers develop as Re increases.

Now that this technique has been demonstrated to be useful in bounding problems of interest, we aim to apply it to determine the complete numerical solution for the upper bound of the long-time-averaged buoyancy flux in stratified plane Couette flow. Our aim is to address several of the outstanding issues associated with the previous study reported in CK01. We wish to determine whether there is any dependence on overall stratification (or indeed on the appropriate fluid diffusivities) of the best possible bound on the buoyancy flux. We also wish to address the extent to which the bound is improved by allowing the background fields to take completely arbitrary form. Furthermore, we are interested in the dependence on Reynolds number of the bounds on mixing parameters, which can only be determined by this full numerical method. Finally, we wish to investigate how the efficiency of the mixing is affected by direct consideration of the best possible bound.

To address these aims, this paper is organized as follows. In § 2, we discuss the appropriate governing equations for stratified plane Couette flow, and formulate the CDH problem. We show that there is a close correspondence between the bounding solutions for the buoyancy flux in stratified plane Couette flow, and the bounding solutions for the dissipation in unstratified Couette flow determined by PK03. We also discuss the numerical method, which is based on the method discussed in detail in PK03. In § 3, we present our results for the flow structures associated with our bounding solutions. We not only discuss the properties, as the external parameters vary, of the long-time-averaged buoyancy flux, as defined in (1.3), but also the mechanical energy dissipation rate, as defined in (1.2). The dissipation is particularly important, as it allows us to consider the 'efficiency' of the mixing that would be associated with the buoyancy flux attaining its bounding value. In § 4, we discuss our results and draw some conclusions.

2. Formulation of the variational problem

In the derivation of the appropriate governing equations, we follow CK01, which considered the same physical system, namely stratified plane Couette flow, in which a layer of fluid is sheared by two infinite parallel plates at $z = \pm d/2$ that are moving with velocities $\mp(\Delta U/2)\,\hat{\boldsymbol{x}}$, respectively. The flow is stratified by requiring that the plates are maintained at constant but different temperatures, so that there is a stable density difference across the layer of $\Delta\rho$.

Assuming that the density variations are sufficiently small so that use of the Boussinesq approximation is appropriate, we use the plate separation d, a characteristic density ρ_0 (where $\Delta\rho/\rho_0 \ll 1$) and the thermal diffusion time scale d^2/κ (κ is the thermal diffusivity) to non-dimensionalize the governing equations, which become:

$$\frac{\partial \boldsymbol{u}}{\partial t} + \boldsymbol{u}\cdot\nabla\boldsymbol{u} + \nabla p - \sigma\nabla^2\boldsymbol{u} + \sigma^2 Re^2 J\rho\,\hat{\boldsymbol{z}} = 0 \qquad (\mathscr{N}\mathscr{S} = 0), \tag{2.1}$$

$$\frac{\partial \rho}{\partial t} + \boldsymbol{u}\cdot\nabla\rho - \nabla^2\rho = 0 \qquad (\mathscr{D} = 0), \tag{2.2}$$

$$\nabla\cdot\boldsymbol{u} = 0. \tag{2.3}$$

In these equations, ρ is the (non-dimensional) difference in the density from ρ_0 scaled by $\Delta\rho$. The appropriate boundary conditions are

$$\boldsymbol{u}\left(x, y, \pm\tfrac{1}{2}, t\right) = \mp\left(\sigma\frac{Re}{2}\right)\hat{\mathbf{x}}, \quad \rho\left(x, y, \pm\tfrac{1}{2}, t\right) = \mp\tfrac{1}{2}, \tag{2.4}$$

where $\boldsymbol{u} = (u_1, u_2, u_3)$. The appropriate non-dimensional groups of the system are the Reynolds number Re, the Prandtl number σ and the (bulk) Richardson number J, defined as:

$$Re = \frac{\Delta U d}{\nu}, \quad \sigma = \frac{\nu}{\kappa}, \quad J = \frac{g\Delta\rho d}{\rho_0(\Delta U)^2}, \tag{2.5}$$

where g is the acceleration due to gravity and ν is the kinematic viscosity.

We define volume averaging and horizontal averaging of some spatially varying quantity q as

$$\langle q(x, y, z)\rangle = \int_{-1/2}^{1/2}\overline{q}\,\mathrm{d}z := \int_{-1/2}^{1/2}\left(\lim_{L_x, L_y\to\infty}\frac{1}{4L_xL_y}\int_{-L_x}^{L_x}\int_{-L_y}^{L_y} q\,\mathrm{d}y\,\mathrm{d}x\right)\mathrm{d}z. \tag{2.6}$$

As discussed in CK01, provided the velocity and density fields are initially square integrable, a number of dynamic balances emerge from the governing equations over long times. Taking the dot product of $\boldsymbol{u}$ with (2.1) and globally averaging gives the long-time kinetic energy balance,

$$\lim_{t\to\infty}\frac{1}{t}\int_0^t\left(\sigma\langle|\nabla\boldsymbol{u}|^2\rangle + \sigma^2Re^2J\langle\rho u_3\rangle + \frac{\sigma^2Re}{2}\left[\left.\frac{\partial\bar{u}}{\partial z}\right|_{z=1/2} + \left.\frac{\partial\bar{u}}{\partial z}\right|_{z=-1/2}\right]\right)\mathrm{d}\tilde{t} = 0. \tag{2.7}$$

Similarly, multiplying (2.2) by ρ yields the entropy flux balance,

$$\lim_{t\to\infty}\frac{1}{t}\int_0^t\left(\langle|\nabla\rho|^2\rangle + \frac{1}{2}\left[\left.\frac{\partial\bar{\rho}}{\partial z}\right|_{z=1/2} + \left.\frac{\partial\bar{\rho}}{\partial z}\right|_{z=-1/2}\right]\right)\mathrm{d}\tilde{t} = 0, \tag{2.8}$$

while multiplying (2.2) by z yields the potential energy balance,

$$\lim_{t\to\infty}\frac{1}{t}\int_0^t\left(1 + \langle\rho u_3\rangle + \frac{1}{2}\left[\left.\frac{\partial\bar{\rho}}{\partial z}\right|_{z=1/2} + \left.\frac{\partial\bar{\rho}}{\partial z}\right|_{z=-1/2}\right]\right)\mathrm{d}\tilde{t} = 0. \tag{2.9}$$

We are interested in maximizing the appropriately non-dimensional averaged buoyancy flux $\mathscr{B}$

$$\mathscr{B} := \lim_{t\to\infty}\frac{1}{t}\int_0^t\sigma^2Re^2J\langle\rho u_3\rangle\,\mathrm{d}\tilde{t} \equiv \lim_{t\to\infty}(1/t)\int_0^t\sigma^2Re^2J(\langle|\nabla\rho|^2\rangle - 1)\,\mathrm{d}\tilde{t}, \tag{2.10}$$

using (2.8) and (2.9). (Note that this definition differs from that used in CK01 by a factor of σ, and is the correct measure of the actual non-dimensional buoyancy flux.) For mathematical convenience, in what follows we actually calculate an upper bound of the quantity $\mathscr{B} + \sigma^2Re^2J$ at fixed σ, Re and J.

We derive the variational problem of interest using the 'background' formulation due to Doering and Constantin (see Doering & Constantin 1992, 1994, 1996; Constantin & Doering 1995) which relies on a fundamental insight of Hopf (1941); as mentioned in § 1, following PK03, we refer to the problem as the CDH problem. We consider the Lagrangian functional $\mathscr{L}$:

$$\mathscr{L} = \lim_{t\to\infty}\frac{1}{t}\int_0^t\left[\sigma^2Re^2J\langle|\nabla\rho|^2\rangle - a\langle\boldsymbol{v}\cdot(\mathscr{N}\mathscr{S})\rangle - \sigma^2Re^2Jb\langle\theta(\mathscr{D})\rangle\right]\mathrm{d}\tilde{t}, \tag{2.11}$$

where ($\mathscr{NS}$) and ($\mathscr{D}$) are the left-hand sides of the Navier–Stokes equations and the density equations (2.1) and (2.2), respectively. (The calculation of CK01 can be recovered from this expression under the transformations:

$$a \to \sigma a_{CK}, \quad b \to \frac{b_{CK}}{\sigma Re^2 J}, \quad \mathscr{L} \to \sigma \mathscr{L}_{CK}, \quad \mathscr{B} \to \sigma \mathscr{B}_{CK}, \tag{2.12}$$

where the subscript 'CK' refers to the quantities as defined in CK01.)

Here, $a\boldsymbol{v}$ and $\sigma^2 Re^2 Jb\theta$ are Lagrange multipliers which formally impose the governing equations. We aim to find the maximum stationary value of $\mathscr{L}$ over all possible $\boldsymbol{u}$, $\boldsymbol{v}$, ρ, θ, a and b, which will then determine the maximum long-time-averaged buoyancy flux. The CDH method relates the Lagrange multipliers $\boldsymbol{v}$ and θ to the physical fields $\boldsymbol{u}$ and ρ, respectively, through one-dimensional time-independent 'background' fields $\phi(z)$ and $\tau(z)$ that satisfy the (inhomogeneous) boundary conditions, i.e.

$$\boldsymbol{u}(\boldsymbol{x}, t) = \phi(z)\hat{\boldsymbol{x}} + \boldsymbol{v}(\boldsymbol{x}, t), \quad \rho(\boldsymbol{x}, t) = \tau(z) + \theta(\boldsymbol{x}, t), \tag{2.13}$$

where

$$\phi = \mp\frac{\sigma Re}{2}, \quad \tau = \mp\tfrac{1}{2}, \quad \boldsymbol{v} = \boldsymbol{0}, \quad \theta = 0 \text{ at } z = \pm\tfrac{1}{2}. \tag{2.14}$$

It is important to appreciate that this decomposition is non-unique, and that the background fields ϕ and τ do not necessarily correspond to horizontal spatial averages of the total flow fields since horizontal averages of the so-called 'fluctuation' fields $\overline{\boldsymbol{v}}$ and $\overline{\theta}$ are allowed to be non-zero. This decomposition into background fields that satisfy the boundary conditions and (incompressible) fluctuation fields that satisfy homogeneous boundary conditions is known as the Hopf decomposition (Hopf 1941).

Since $\boldsymbol{v}$ and θ are related to $\boldsymbol{u}$ and ρ, optimization of $\mathscr{L}$ as defined in (2.11) can be shown to impose only mean streamwise momentum balance, total power balance, entropy flux balance and the mean heat balance (with Lagrange multipliers $-a\phi$, a, $\sigma^2 Re^2 Jb$ and $-\sigma^2 Re^2 Jb\tau$, respectively). Essentially, if ϕ and τ can be chosen so that $\mathscr{L}$ has a maximum over all possible fluctuation fields $\boldsymbol{v}$ and θ, then this value of $\mathscr{L}$ must lead to a rigorous upper bound on the buoyancy flux, as any actually realizable $\boldsymbol{u}$ and ρ that satisfy the actual governing equations must be accessible by some appropriate choice of $\boldsymbol{v}$ and θ. Minimizing the maximum over all possible ϕ, τ, a and b then yields the best possible upper bound (see Kerswell 1998 for more discussion of the underlying principles).

We assume that the stated problem of interest is well-posed, and so we drop the long-time averages. As shown in CK01 and PK03, it is appropriate to separate the streamwise component of the fluctation velocity v_1 and the fluctuation density θ into mean parts $\overline{v_1}(z)$ and $\overline{\theta}(z)$ and meanless parts $\hat{v}_1(x, y, z)$ and $\hat{\theta}(x, y, z)$ such that $\overline{\hat{v}_1} = \overline{\hat{\theta}} = 0$. Then, a necessary condition for an extremum of $\mathscr{L}$ to exist is that $\mathscr{L}$ satisfies ten Euler–Lagrange equations: with respect to the Lagrange multipliers a and b; the background fields ϕ and τ; the horizontally averaged streamwise fluctuation velocity $\overline{v_1}$; the three components of the meanless fluctuation velocity field $\hat{\boldsymbol{v}}$; the horizontally averaged fluctuation density field $\overline{\theta}$; and the meanless fluctuation density field $\hat{\theta}$. The Euler–Lagrange equations for the mean fluctuation quantities $\overline{v_1}$ and $\overline{\theta}$ can be straightforwardly solved to yield

$$\overline{\boldsymbol{v}} = -\tfrac{1}{2}(\phi + \sigma Rez)\hat{\boldsymbol{x}}, \quad \overline{\theta} = -\frac{(b-2)}{2(b-1)}(\tau + z). \tag{2.15}$$

Using these expressions, the remaining Euler–Lagrange equations are equivalent to the set of equations:

$$\frac{\delta\mathscr{L}}{\delta a} := 0 \to \frac{a\sigma}{4}\langle(\phi' + \sigma Re)^2\rangle - a\sigma^2 Re^2 J\langle\hat{v}_3\hat{\theta}\rangle - (b-1)\sigma^2 Re^2 J\langle|\nabla\hat{\theta}|^2\rangle = 0, \quad (2.16)$$

$$\frac{\delta\mathscr{L}}{\delta b} := 0 \to \frac{b^2}{(b-2)}\langle(\overline{\theta}')^2\rangle + (b-2)\langle|\nabla\hat{\theta}|^2\rangle + a\langle\hat{v}_3\hat{\theta}\rangle = 0, \quad (2.17)$$

$$\frac{\delta\mathscr{L}}{\delta\phi} := 0 \to \tfrac{1}{2}\sigma(\phi' + \sigma Re) - \overline{\hat{v}_1\hat{v}_3} + \langle\hat{v}_1\hat{v}_3\rangle = 0, \quad (2.18)$$

$$\frac{\delta\mathscr{L}}{\delta\tau} := 0 \to \frac{b\overline{\theta}'}{(b-2)} - \langle\hat{v}_3\hat{\theta}\rangle + \overline{\hat{v}_3\hat{\theta}} = 0, \quad (2.19)$$

$$\frac{\delta\mathscr{L}}{\delta\hat{\mathbf{v}}} := 0 \to 2a\sigma\nabla^2\hat{\mathbf{v}} - a\phi'\begin{bmatrix}\hat{v}_3\\0\\\hat{v}_1\end{bmatrix} - (b\tau' + a)\sigma^2 Re^2 J\hat{\theta}\hat{\mathbf{z}} - a\nabla\hat{p} = \mathbf{0}, \quad (2.20)$$

$$\frac{\delta\mathscr{L}}{\delta\hat{\theta}} := 0 \to 2(b-1)\sigma^2 Re^2 J\nabla^2\hat{\theta} - (b\tau' + a)\sigma^2 Re^2 J\hat{v}_3 = 0, \quad (2.21)$$

where $(.)' = (\mathrm{d}/\mathrm{d}z)(.)$, and cubic terms of the form $\langle\phi'\hat{v}_1\hat{v}_3\rangle$ and $\langle\overline{\theta}'\hat{v}_3\hat{\theta}\rangle$ have been eliminated by taking the spatial average of the dot product of (2.20) with $\hat{\mathbf{v}}$ and the spatial average of the product of (2.21) with $\hat{\theta}$, respectively.

A relationship between a and b can be derived straightforwardly by remembering the conditions for entropy flux balance and potential energy balance, i.e. (2.8) and (2.9). Noting that the homogeneous boundary conditions (2.14) imply that $\langle\overline{\theta}'\rangle = 0$, these equations can be shown to be equivalent to

$$\langle\hat{v}_3\hat{\theta}\rangle = \frac{b^2\langle(\overline{\theta}')^2\rangle}{(b-2)^2} + \langle|\nabla\hat{\theta}|^2\rangle. \quad (2.22)$$

Substituting (2.22) into (2.17) implies that, if the buoyancy flux contribution $\langle\hat{v}_3\hat{\theta}\rangle$ is non-zero,

$$b = (2-a). \quad (2.23)$$

Therefore, it is possible to show that the quantity $\mathscr{L}$ defined in (2.11) takes the form

$$\mathscr{L} = \frac{(2-a)^2(1-a)\sigma}{a^2}\langle(\overline{\theta}')^2\rangle + \sigma^2 Re^2 J + \frac{a\sigma}{4}\langle(\phi' + \sigma Re)^2\rangle - \mathscr{H}_{\phi,\tau,a}(\hat{\mathbf{v}},\hat{\theta}), \quad (2.24)$$

where

$$\mathscr{H}_{\phi,\tau,a}(\hat{\mathbf{v}},\hat{\theta}) := a\sigma\langle\|\nabla\hat{\mathbf{v}}\|^2\rangle + a\langle\phi'\hat{v}_1\hat{v}_3\rangle + (1-a)\sigma^2 Re^2 J\left[\langle|\nabla\hat{\theta}|^2\rangle - 2\langle\hat{v}_3\hat{\theta}\rangle + \frac{(2-a)}{a}\langle\overline{\theta}'\hat{v}_3\hat{\theta}\rangle\right]. \quad (2.25)$$

For a stationary value of $\mathscr{L}$ to be an upper bound, it is necessary for the so-called 'spectral constraint' to be satisfied, i.e.

$$\mathscr{H}_{\phi,\tau,a}(\hat{\mathbf{v}},\hat{\theta}) \geqslant 0, \quad (2.26)$$

for all $\hat{\theta}$ and incompressible $\hat{\mathbf{v}}$ that satisfy homogeneous boundary conditions at $z = \pm 1/2$. Clearly, a necessary condition for the spectral constraint to be satisfied is for $0 \leqslant a \leqslant 1$. The Euler–Lagrange equations for $\hat{\mathbf{v}}$ and $\hat{\theta}$ (i.e. (2.20) and (2.21)) imply

that $\mathscr{H}_{\phi,\tau,a}(\hat{\boldsymbol{v}},\hat{\theta})=0$ at every stationary point of $\mathscr{L}$. However, it is only at the largest (and unique) stationary value that the spectral constraint (2.26) is satisfied. Therefore, if we can identify a solution to the Euler–Lagrange equations (2.16)–(2.21) that satisfy the associated spectral constraint (2.26), then we will indeed have identified the (best possible) upper bound consistent with the imposed constraints.

2.1. *The limit* $a \to 1$

The particular limit of $a \to 1$ is appealing, as it is consistent with, and generalizes, the previous conservative result in CK01, where, as discussed in § 1, attention was restricted to flows where the meanless parts $\hat{\boldsymbol{v}}$ and $\hat{\theta}$ were required to be exactly zero, and only piecewise linear background fields were allowed. In this case, from (2.24), the upper bound on $\mathscr{L}$ (i.e. when $\mathscr{H}=0$) takes the value

$$\mathscr{L} \leqslant \mathscr{L}_{max} = \mathscr{B}_{max} + \sigma^2 Re^2 J = \sigma^2 Re^2 J + \tfrac{1}{4}\sigma\langle(\phi' + \sigma Re)^2\rangle, \tag{2.27}$$

also defining an upper bound on the long-time-averaged buoyancy flux $\mathscr{B} \leqslant \mathscr{B}_{max}$.

Furthermore, in the limits $a \to 1$, and hence $b \to 1$ from (2.23), it is possible to establish that $\tau = -z$. Therefore, assuming for the moment that the limit $a \to 1$ is consistent with the Euler–Lagrange equations (2.16)–(2.21), optimizing solutions to the Euler–Lagrange equations have linear background density profiles. This implies that the velocity field decouples from the density field in $\mathscr{L}$ and $\mathscr{H}_{\phi,\tau,a}(\hat{\boldsymbol{v}},\hat{\theta})$ from (2.24) and (2.25). Furthermore, both $\mathscr{L}$ and $\mathscr{H}$ are independent of the meanless fluctuation density field $\hat{\theta}$.

Indeed, under this limit, $\hat{\boldsymbol{v}}$, $\overline{v_1}$ and ϕ can be completely determined by (2.15), (2.18) and (2.20). This last equation becomes

$$2\sigma\nabla^2\hat{\boldsymbol{v}} - \phi'\begin{bmatrix}\hat{v}_3\\0\\\hat{v}_1\end{bmatrix} - \nabla\hat{p} = \boldsymbol{0}, \tag{2.28}$$

with pressure being determined naturally by the requirement that $\hat{\boldsymbol{v}}$ is incompressible. For these solutions to lead to an upper bound, it is necessary for the associated ϕ to satisfy the highly simplified spectral constraint

$$\mathscr{H}_{\phi}(\hat{\boldsymbol{v}}) = \langle\|\nabla\hat{\boldsymbol{v}}\|^2\rangle + \langle\phi'\hat{v}_1\hat{v}_3\rangle \geqslant 0, \tag{2.29}$$

for all incompressible $\hat{\boldsymbol{v}}$ with homogeneous boundary conditions.

Equations (2.15), (2.18), (2.28) and (2.29) are very closely related to those considered in PK03 for identifying an upper bound for the mechanical energy dissipation rate. Indeed, under the transformations

$$\frac{\phi}{\sigma} \to \lambda\phi_{PK}, \quad Re \to \lambda Re_{PK}, \quad \frac{\overline{v_1}}{\sigma} \to \frac{\lambda}{(2-\lambda)}\overline{v_1}_{PK}, \quad \frac{\hat{\boldsymbol{v}}}{\sigma} \to \hat{\boldsymbol{v}}_{PK}, \tag{2.30}$$

where the subscript '*PK*' refers to the quantities as defined in the PK03, and λ is their parameter defined

$$\lambda \equiv 2 - \frac{\langle\|\nabla\hat{\boldsymbol{v}}_{PK}\|^2\rangle}{Re_{PK}\langle\hat{v}_{1PK}\hat{v}_{3PK}\rangle} = \frac{2Re\langle\hat{v}_1\hat{v}_3\rangle}{Re\langle\hat{v}_1\hat{v}_3\rangle + \langle\|\nabla\hat{\boldsymbol{v}}\|^2\rangle}, \tag{2.31}$$

(2.15), (2.18), (2.28) and (2.29) are exactly equivalent to equations (2.11), (2.13*b*), (2.13*c*) and (2.15), respectively, of PK03.

Both the bounding functional $\mathscr{L}$ in this paper and in PK03 essentially involve imposing mean streamwise momentum balance, and so the agreement in the structure

of the equations determining $\hat{\boldsymbol{v}}$ (i.e. (2.28) and (2.13*c*) of PK03) follows naturally when $a = 1$, since there is no coupling between the velocity and the density fields. The primary difference between the two problems is that PK03 generated a bound on the mechanical energy dissipation rate, as opposed to the long-time-averaged buoyancy flux considered here. This difference manifests itself mathematically in the different forms of the mean fluctuation velocities $\overline{v_1}$ and $\overline{v_1}_{PK}$ defined in (2.30). Taking this difference into account then yields straightforwardly the simple correspondence between the equations determining ϕ and ϕ_{PK}, i.e. (2.18) and (2.13*b*) of PK03.

Therefore, under the limit $a \to 1$, the stationary solutions ϕ and $\hat{\boldsymbol{v}}$ for the problem of interest, i.e. generating a rigorous bound on the long-time average of the buoyancy flux in a stratified Couette flow, correspond exactly in structure to the bounding solutions that maximize the mechanical energy dissipation rate in an equivalent flow with a Reynolds number lower by a factor of λ as defined in (2.31). As discussed in PK03, λ varies between one at the energy stability Reynolds number, Re_{ES} (where there exists an incompressible $\hat{\boldsymbol{v}}$, such that $Re_{ES}\langle \hat{v}_1 \hat{v}_3 \rangle = \langle \|\boldsymbol{\nabla}\hat{\boldsymbol{v}}\|^2 \rangle$) and 3/2 as $Re \to \infty$ (see Joseph 1976). From the results of PK03, we know that (2.18) and (2.28) do, in general, have a solution that satisfies the appropriate spectral constraint (2.29). Therefore, it is indeed possible to construct a consistent solution to the Euler–Lagrange equations (2.16)–(2.21) with $a = 1$ satisfying the appropriate spectral constraint. This justifies our initial assumption of $a = 1$, and allows the substantial simplification of $a = b = 1$.

2.2. *Numerical solution technique*

To construct the upper bound solution, all we need to do is to solve (2.18) and (2.28) (essentially the Euler–Lagrange equations for variations with respect to ϕ and (incompressible) $\hat{\boldsymbol{v}}$, respectively) to determine $\phi(Re)$ and $\hat{\boldsymbol{v}}(Re)$ for the bounding solution at our particular Re. We can then use (2.31) as a diagnostic equation to determine λ, and hence the equivalent Reynolds number $Re_{PK} = Re/\lambda$ as defined in (2.30).

To solve (2.18) and (2.28), we closely follow the numerical procedure described in detail in PK03. The equations are solved numerically using pseudospectral collocation (Boyd 2001), assuming that the bounding solution has no streamwise variation, $\partial/\partial x = 0$ (Busse 1969*a*, 1970). We expand the background and fluctuation fields in Chebyshev polynomials in the vertical direction to ensure adequate resolution in the expected boundary layers. Spanwise variation is captured by a Fourier decomposition. We use the numerical continuation package PITCON (Rheinboldt & Burkhardt 1983*a*, *b*) to continue the solution of the Euler–Lagrange equations (2.18) and (2.28) away from the laminar solution $\phi_l = -\sigma Re z$, $\tau = -z$, $\hat{\theta} = 0$, $\boldsymbol{v} = \boldsymbol{0}$, which ceases to be a global attractor at the energy stability Reynolds number $Re_{ES} = 82.65$ (Joseph 1976). As discussed by PK03, at Re_{ES}, a non-trivial incompressible fluctuation subfield $\hat{\boldsymbol{v}}^{(1)}$ with a given spanwise wavenumber k_1 marginally satisfies the laminar spectral constraint (2.29) with $\phi' = \phi_l' = -\sigma Re$. This mode is then used as a starting point by PITCON, which iterates to a non-trivial solution at higher Re. This bifurcation occurs at the same Reynolds number as in PK03, independently of bulk Richardson number J, since at Re_{ES} the parameter $\lambda = 1$, (as defined in (2.31)) and so there is an exact correspondence between the properties of both problems.

For all solutions to the Euler–Lagrange equations (2.18) and (2.28) determined by continuation as we iterate to larger Re, we ensure that the spectral constraint (2.29) remains satisfied by monitoring an eigenvalue problem. As discussed in PK03, the requirement that $\mathscr{H}$ be positive semi-definite can be shown to be equivalent to solving a linear eigenvalue problem for a three vector subfield $\boldsymbol{V} = (V_1, V_2, V_3)$ over a

particular space of functions Ψ defined as

$$\Psi = \left\{ \boldsymbol{V} \middle| kV_2 + V_3' = 0, \bar{\boldsymbol{V}} = \boldsymbol{0}, \boldsymbol{V}\left(z = \pm\tfrac{1}{2}\right) = 0 \right\}, \tag{2.32}$$

for a given k, where k is the spanwise wavenumber of the subfield $\boldsymbol{V}$. Then, requiring the spectral constraint to be satisfied is equivalent to requiring that solutions $\boldsymbol{V} \in \Psi$ (which are forced to be incompressible) to the linear eigenvalue problem

$$2\sigma(\boldsymbol{V}'' - k^2\boldsymbol{V}) - \phi' \begin{pmatrix} V_3 \\ 0 \\ V_1 \end{pmatrix} - \nabla\hat{p} = \mu\boldsymbol{V}, \tag{2.33}$$

have eigenvalues $\mu \leqslant 0$ for all real values of k.

In particular, for the bounding solution $\hat{\boldsymbol{v}}^{(1)}$ at the energy stability Reynolds number Re_{ES}, $\bar{\mu}$ has a single maximum of zero at $k_1 = 3.117$. The solution is continued as Re increases, leading to a variation of ϕ away from its laminar value. As discussed in more detail in PK03, we extend the solution to include further fluctuation subfields every time a new local maximum in $\bar{\mu}(k)$ threatens to break through the x-axis, and so we can identify the bifurcation structure of the bounding solution to higher and higher Re.

3. Results

From (2.27), the scaling of $\mathscr{B}_{max}$ is completely determined by the scaling of ϕ' as Re increases. This scaling can be easily identified since, as noted above, the structure of both the background velocity field ϕ and the meanless fluctuation velocity field $\hat{\boldsymbol{v}}$ are determined by equations that can be directly related to the equations solved by PK03. PK03 demonstrated that the bound on the mechanical energy dissipation rate $\mathscr{E}$ took the form

$$\mathscr{E} \equiv \langle \|\nabla \boldsymbol{u}_{PK}\|^2 \rangle \leqslant \mathscr{E}_{max} = \frac{\lambda^2}{4(\lambda - 1)} \langle (\phi'_{PK} + Re_{PK})^2 \rangle + Re_{PK}^2, \tag{3.1}$$

where, quite naturally, kinematic viscosity ν rather than thermal diffusivity κ was used in the characteristic time scale used for non-dimensionalization, and as before, the subscript PK denotes quantities as defined in PK03. They showed that

$$\hat{\mathscr{E}}_{max} = \frac{\mathscr{E}_{max}}{Re_{PK}^3} \simeq 0.008553, \tag{3.2}$$

as $Re_{PK} \to \infty$, and hence $\lambda \to 3/2$.

Since, from (2.27), $\mathscr{B}_{max}$ can be related to $\langle (\phi' + \sigma Re)^2 \rangle$, using the transformations given in (2.30), (3.1) and (3.2) imply that

$$\hat{\mathscr{B}}_{max} \equiv \frac{\mathscr{B}_{max}}{\sigma^3 Re^3} = \frac{(\lambda - 1)}{\lambda^3} \left(\hat{\mathscr{E}} - \frac{1}{Re_{PK}} \right) \simeq 0.001267, \tag{3.3}$$

as $Re \to \infty$ since $\lambda \to 3/2$. (Since we use the thermal diffusivity κ to non-dimensionalize our equations, $\mathscr{B}_{max} = O(\sigma^3 Re^3)$ is equivalent to the upper bound on the dimensional buoyancy flux $\mathscr{B}^*_{max} = O(\Delta U^3/d)$).

In figure 1(a), we plot the variation of $\hat{\mathscr{B}}_{max}$ with Re. We also mark (with a dashed line) the expected asymptotic value of 0.001267, and it is apparent that the upper bound on the buoyancy flux increases from zero monotonically at the energy stability point $Re_{ES} = 82.65$ and then converges towards the asymptotic value. The bound on $\hat{\mathscr{B}}_{max}$ is completely independent of both the overall stratification, and the physical

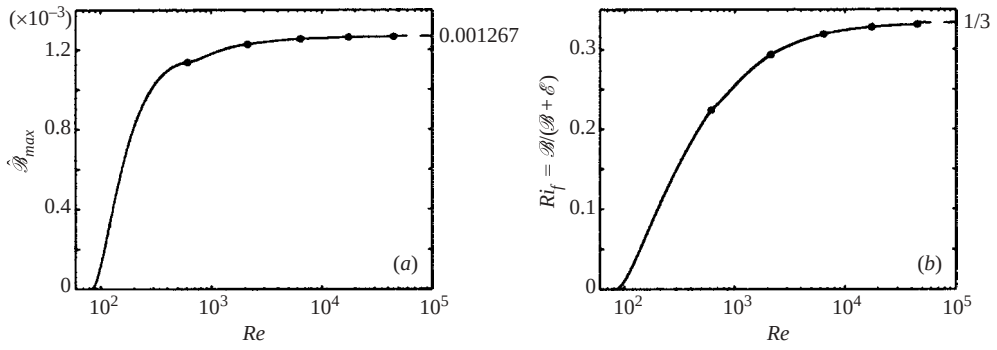

FIGURE 1. (*a*) Variation of the scaled upper bound $\hat{\mathscr{B}}_{max}$ on the long-time-averaged buoyancy flux as defined in (3.3) with *Re*. The predicted asympotic value at high *Re* is marked with a dashed line. The bifurcation points at which new spanwise wavenumbers enter the solution are marked with circles. Note how these points are close to evenly spaced with log(*Re*), exhibiting the expected self-similarity. (*b*) Variation of flux Richardson number Ri_f as defined in (3.6) against *Re* for the solutions corresponding to the upper bound $\mathscr{B}_{max}$ in the long-time-averaged buoyancy flux. The aysmptotic value at large *Re* of 1/3 is marked with a dashed line.

properties of the fluid, since it is independent of J and σ. Furthermore, though the scaling is the same as that determined by the consideration of piecewise linear background fields and zero meanless fluctuations in CK01, the numerical coefficient has been reduced by a factor of 8.68, from $1/(64\sqrt{2}) = 0.011$ to 0.001267.

We are also interested in the mixing efficiency, or equivalently the flux Richardson number Ri_f, as defined in (1.3) associated with the bounding solution. To determine Ri_f for the bounding solutions, we must calculate the (non-dimensional) mechanical energy dissipation rate associated with the bounding solutions $\mathscr{E}_B$, defined as

$$\mathscr{E}_B = \sigma \langle \|\nabla \boldsymbol{u}\|^2 \rangle = \sigma \langle (\overline{u_1}')^2 \rangle + \sigma \langle \|\nabla \hat{\boldsymbol{v}}\|^2 \rangle, \tag{3.4}$$

where $\overline{u_1} = \phi + \overline{v_1}$ is the mean horizontal velocity profile, and ϕ and $\hat{\boldsymbol{v}}$ are determined from the bounding solutions for the buoyancy flux. For the bounding solutions, it can be established that

$$\mathscr{E}_B = \frac{\sigma}{4(\lambda - 1)} \langle (\phi' + \sigma Re)^2 \rangle + \sigma^3 Re^2 = \frac{\mathscr{B}_{max}}{\lambda - 1} + \sigma^3 Re^2, \tag{3.5}$$

and so the flux Richardson number Ri_f is given by

$$Ri_f = \frac{\mathscr{B}_{max}}{\mathscr{B}_{max} + \mathscr{E}_B} = \frac{\mathscr{B}_{max}}{\sigma^3 Re^2 + \frac{\lambda}{(\lambda - 1)} \mathscr{B}_{max}} \to \frac{\lambda - 1}{\lambda} \to \tfrac{1}{3} \quad \text{as} \quad Re \to \infty. \tag{3.6}$$

As for the other quantities of interest that we have considered, this implies that Ri_f depends only on the Reynolds number for flows that attain the upper bound on the long-time-averaged buoyancy flux. This observation is at variance with the observed dependence on J of Ri_f for a range of experimental and numerical investigations (see Linden 1979; Fernando 1991; Peltier & Caulfield 2003 for reviews). In figure 1(*b*), we plot the flux Richardson number for these bounding solutions as a function of *Re*.

The flow adjusts so that there is a partition of the energy input through the shear forcing at the boundaries into three equal (to leading order) parts: the dissipation due to the mean velocity; the dissipation due to the meanless fluctuation velocity; and the buoyancy flux of the flow. (The contribution from the meanless fluctuation velocity appears to be the fundamental reason why the predicted mixing efficiency is less than

that presented in CK01, where $Ri_f \to 1/2$ as $Re \to \infty$, and the meanless fluctuation velocity was assumed to be zero.)

The asymptotic value of the flux Richardson number for the bounding solutions $Ri_f \to 1/3$ is still substantially larger than the commonly inferred values of $Ri_f \sim 0.15{-}0.25$. However, as is apparent in figure 1(*b*), for intermediate values of $Re \sim 1000$, $Ri_f \sim 0.15 - 0.25$. Since the conventional parameterization is based on experimental and numerical observations at moderate Re, it is at least suggestive that the mixing efficiency parameterizations should be adjusted to allow for larger values of Re, which is consistent with the recent large-scale observations of Pardyjak *et al.* (2002).

Also shown in figures 1(*a*) and 1(*b*) with circles are the values of Re at which wavenumber bifurcations occur, when, as discussed above, extra subfields enter the solution so that the spectral constraint remains satisfied. The bifurcation points naturally correspond exactly to those reported in PK03, when the transformations defined by (2.30) are used, for the appropriate value of λ as defined in (2.31). (We have presented our results to one less bifurcation than PK03, as the aysmptotic properties of the solution are already apparent.) Although the approach of λ to its asymptotic value 3/2 is non-smooth (see PK03) λ approaches 3/2 quite quickly, and is within 1% of its asymptotic value for all $Re > 1300$. This implies that, to a good approximation, the $\hat{\boldsymbol{v}}$ and ϕ that we have identified correspond to $\hat{\boldsymbol{v}}$ and ϕ in an unstratified flow with Reynolds number 33% smaller. Also, the structure of the various z-dependent subfields for the fluctuation velocity (and pressure) correspond to those considered in PK03, and, in particular, they may be thought of as having the expected self-similar structure as assumed by Busse's (1970) multiple boundary-layer analysis (see PK03 for more discussion).

As noted in PK03, the mean velocity gradient (for their problem of maximizing the long-time-averaged mechanical dissipation rate in unstratified plane Couette flow) tends towards $-Re/4$ in the interior of the flow, corresponding to ϕ_{PK} being constant (and zero) throughout the interior of the flow domain. Dimensionally, this gradient corresponds to $-\Delta U/4$. However, the mean velocity profile for the solutions that maximize the long-time averaged buoyancy flux in stratified plane Couette flow has a different interior gradient, which, within this non-dimensionalization, corresponds to $-\sigma Re/2$. This agrees with the value determined for the piecewise linear profiles considered in CK01, and implies a non-trivial difference in the interior between stratified and unstratified flows. Dimensionally, this gradient corresponds to $-\Delta U/2$, dependent naturally only on the overall velocity difference of the flow.

This difference in mean profiles manifests itself when we attempt to identify a correspondence between the mechanical energy dissipation rate $\mathscr{E}_B$, as defined in (3.4), associated with an upper bound on the buoyancy flux for the stratified bounding solutions and the upper bound $\mathscr{E}_{max}$ for the unstratified bounding solutions. Substituting (2.30) into (3.5), we obtain

$$\mathscr{E}_B = \sigma^3\lambda^2 Re_{PK}^2 + \frac{\sigma^3\lambda^2}{4(\lambda-1)}\langle(\phi'_{PK} + Re_{PK})^2\rangle, \tag{3.7}$$

$$= \sigma^3\left[\mathscr{E}_{max} + (\lambda^2-1)Re_{PK}^2\right], \tag{3.8}$$

and so the scaled dissipation $\hat{\mathscr{E}}_B$ is given by

$$\hat{\mathscr{E}}_B = \frac{\mathscr{E}_B}{\sigma^3 Re^3} = \frac{\left[\mathscr{E}_{max} + (\lambda^2-1)Re_{PK}^2\right]}{\lambda^3 Re_{PK}^3} = \frac{\hat{\mathscr{E}}_{max}}{\lambda^3} + \frac{(\lambda^2-1)}{Re_{PK}}, \tag{3.9}$$

$$\to \frac{2^3}{3^3}(0.008553) = 0.002534 \quad \text{as} \quad Re \to \infty. \tag{3.10}$$

Therefore, the dissipation is substantially less (by a factor 8/27) than the upper bound for the flow when it is unstratified. This is because the flow which bounds the buoyancy flux corresponds to an unstratified flow with smaller Reynolds number and hence, naturally, less dissipation. The difference $(\lambda^2-1)/Re_{PK}$ between the two expressions is essentially a laminar contribution from the mean velocity field, arising because of the differences in mean gradient, particularly in the interior of the flow domain. However, the significance of the difference of the interior shear between the two solutions should be treated with caution, since, as discussed in detail in PK03, the mean profile for the bounding solutions does not appear to agree well with physically realized flows.

Since the mixing within the bounding flow appears to be independent of J, a natural question to ask is how the flow adjusts to allow the mixing to be sustained at arbitrarily high stratification. When $a=1$, since as already noted the functional $\mathscr{L}$ does not depend on $\hat{\theta}$, the meanless fluctuation density field cannot be determined uniquely. However, certain important constraints on the density field can be identified. Substitution of (2.16) into the Euler–Lagrange equation (2.19) for variations with respect to τ yields

$$\overline{\theta}' = \overline{\hat{v}_3\hat{\theta}} - \frac{\sigma}{4\sigma^2 Re^2 J}\langle(\phi' + \sigma Re)^2\rangle, \tag{3.11}$$

which implies, since $\hat{\boldsymbol{v}}$ is incompressible, that

$$\overline{\theta}''|_{z=\pm 1/2} = \overline{\theta}'''|_{z=\pm 1/2} = 0. \tag{3.12}$$

Although not imposed directly by the equations, it is also reasonable to require that the mean density profile is statically stable and so to require that $\overline{\theta}' \leqslant 1$ everywhere, allowing the possibility of $\overline{\theta}' = 1$ as $z \to 0$, and hence the development of a well-mixed layer in the interior of the flow. (This reasonable condition is not imposed by the problem formulation, and does not affect the principal results.) Finally, the density fluctuations are required to satisfy the energy constraint (2.22), which when $a=b=1$, takes the simple form

$$\langle\hat{v}_3\hat{\theta}\rangle = \langle(\overline{\theta}')^2\rangle + \langle|\nabla\hat{\theta}|^2\rangle. \tag{3.13}$$

It is always possible to construct density profiles that satisfy these criteria.

In figure 2, we plot (with solid lines) vertical profiles for the mean alongstream velocity $\overline{u_1}$ at the Reynolds number of the second, third, fourth and fifth bifurcation points. We also plot (with dashed lines) constructed characteristic mean density profiles $\bar{\rho}(z) = \tau + \bar{\theta}$ satisfying $\tau = -z$, (3.11), and the boundary conditions (3.12) for appropriately chosen meanless fluctuation density fields $\hat{\theta}$ satisfying the constraint (3.13). From these equations, it is clear that the structure (in particular the magnitude) of the density profile does depend on J and σ. For simplicity, we have chosen to set $J=1$ and $\sigma=1$, though this does not change our conclusions substantially. We only plot half the channel $1/2 \leqslant z \leqslant 0$ because of the symmetry of the flow structures about the midplane. In general, as noted by PK03, as Re increases, the mean velocity profile becomes more and more tightly constrained in thinner and thinner boundary layers. The predicted $-\sigma Re/2$ gradient in the interior of the flow for the mean velocity gradient is readily apparent, particularly at large Re.

The constructed density profiles for the flows under consideration also follow the same general structure, with thinner and thinner boundary layers as Re increases. A critical aspect is that, in all cases, the velocity boundary layer is embedded within the density boundary layer (as also observed in CK01). This means that the local

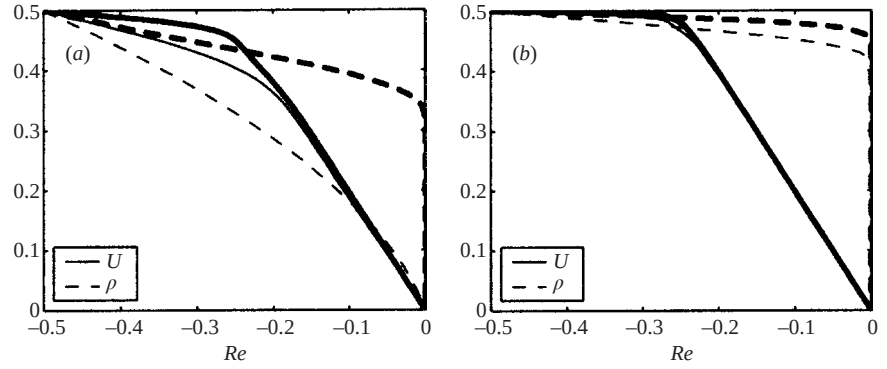

FIGURE 2. Variation with height z of mean velocity profile (plotted with a solid line) and typical mean density profile (dashed line) for flows corresponding to an upper bound in the long-time-averaged buoyancy flux with Reynolds numbers at the four bifurcation points (*a*) $Re = 609$ (thin lines) and $Re = 2119$ (thick lines); (*b*) $Re = 6359$ (thin lines) and $Re = 17\,480$ (thick lines).

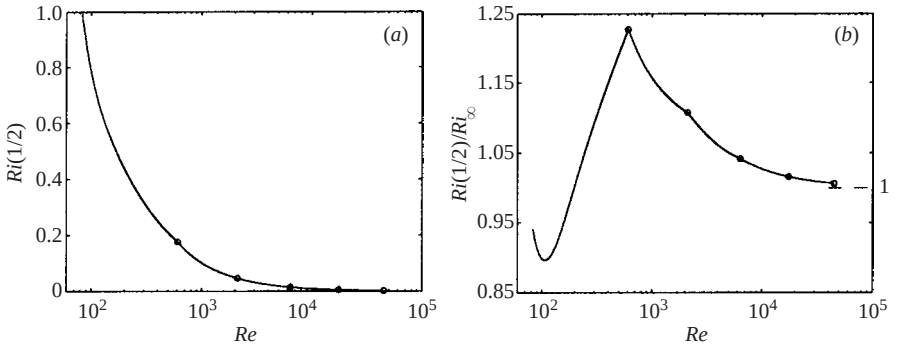

FIGURE 3. (*a*) Variation with Reynolds number of the gradient Richardson number at the boundaries $Ri(1/2)$ of the solutions corresponding to the upper bound of the buoyancy flux in stratified plane Couette flow. (*b*) Variation with Re of $Ri(1/2)/Ri_\infty$ where Ri_∞ is the asymptotic value of $Ri(1/2)$ defined in (3.18).

gradient Richardson number $Ri(z)$, defined as

$$Ri(z) := \frac{-\dfrac{g}{\rho_0}\dfrac{\mathrm{d}\bar{\rho}^*}{\mathrm{d}z^*}}{\left(\dfrac{\mathrm{d}\overline{u_1^*}}{\mathrm{d}z^*}\right)^2} = -\sigma^2 Re^2 J \frac{\mathrm{d}\bar{\rho}}{\mathrm{d}z}\left(\frac{\mathrm{d}\bar{u}_1}{\mathrm{d}z}\right)^{-2}, \tag{3.14}$$

where asterisks denote dimensional quantities, has a certain generic structure in all cases. In the interior of the flow, where the density is constant at its mean value, and the velocity has the characteristic $-\sigma Re/2$ shear as discussed above, $Ri(z) = 0$. There is an intermediate region nearer to the wall that is in the density boundary layer yet outside the velocity boundary layer, where Ri grows to larger values. Finally, there is always an inner region within both the velocity and density boundary layers, where $Ri(z)$ drops to very low values.

Indeed, irrespective of the particular constructed density profile, $Ri(z)$ right at the boundaries of the flow is completely determined. In figure 3(*a*), we plot the variation with Re of the gradient Richardson number at the boundaries of the flow,

i.e. $Ri(\pm 1/2)$. It is clear that this quantity decreases markedly with Reynolds number. Using $\tau' = -1$, (2.16), (3.11), (2.27), and the fact that the fluctuation fields are zero on the boundaries, the mean density gradient at $z = \pm 1/2$ can be shown to be

$$-\sigma^2 Re^2 J \left.\frac{\mathrm{d}\bar{\rho}}{\mathrm{d}z}\right|_{z=\pm 1/2} = \mathscr{B}_{max} + \sigma^2 Re^2 J. \tag{3.15}$$

Similarly, using (2.15), (2.18) and (2.31)

$$\left.\frac{\mathrm{d}\overline{u_1}}{\mathrm{d}z}\right|_{z=\pm 1/2} = \frac{\lambda}{\sigma^2 Re(\lambda - 1)} \mathscr{B}_{max} - \sigma Re, \tag{3.16}$$

and so, for the upper bounding solutions

$$Ri\left(\frac{\pm 1}{2}\right) = \frac{\hat{B}_{max}\sigma^3 Re^3 + \sigma^2 Re^2 J}{\left(\dfrac{\lambda \sigma Re^2}{(\lambda - 1)} \hat{B}_{max} + \sigma Re\right)^2}, \tag{3.17}$$

$$\rightarrow Ri_\infty = \frac{(\lambda - 1)^2 \sigma}{\lambda^2 \hat{\mathscr{B}}_{max} Re} = \frac{87.69\sigma}{Re} \quad \text{as} \quad Re \rightarrow \infty. \tag{3.18}$$

Therefore, owing to the particular structure of the boundary conditions, $Ri(z)$ approaches very small values $Ri_\infty = O(\sigma/Re)$ at the boundaries, irrespective of the bulk stratification, as quantified through J. This is qualitatively similar to the behaviour observed for piecewise linear profiles as considered by CK01. In figure 3(*b*), we plot the ratio $Ri(1/2)/Ri_\infty$, as defined in (3.18) against Re. Provided the Prandtl number is sufficiently small, this result implies that near the flow boundaries the local Richardson number drops to extremely small values. Therefore, as assumed by Townsend (1958), it is reasonable to suppose that sustained turbulent motions near the boundaries are little affected by the stratification. Essentially, to leading order, the density field can act as a passive scalar advected by the turbulence within the flow, hence enabling the largest possible buoyancy flux consistent with the flow boundary conditions.

4. Discussion and conclusions

We have derived the complete solution to the CDH problem for bounding the long-time-averaged buoyancy flux in plane stably stratified Couette flow, up to a sufficiently high Reynolds number $Re = 45\,005$ and wavenumber bifurcation to identify an asymptotic value of the bound, $\hat{B}_{max} = 0.001267$ (as defined in (3.3)). This bound improves the previous result of CK01 (based on piecewise linear velocity profiles) by a factor of 8.7. This bounding solution is independent of both the overall stratification of the Couette flow, and the Prandtl number of the fluid. Physically, this independence appears to be due to the fact that the bounding solution always develops velocity boundary layers that are thinner than the density boundary layers. This coupled boundary-layer structure leads to very low local values of the gradient Richardson number near the wall. Mathematically, it manifests itself in the fact that the overall strength of the density field does not directly affect the structure of the velocity fluctuations, because of the particular values of the Lagrange multipliers ($a = b = 1$) predicted to be associated with stationary values of the buoyancy flux functional $\mathscr{L}$.

A further effect of the lack of a direct coupling between the density field and the velocity field is that there is a correspondence between our results and those reported

in PK03. For the bounding solutions for the meanless fluctuation velocity $\hat{\boldsymbol{v}}$ and background velocity ϕ, we show that there is an exact correspondence between the stratified Couette flow, and an unstratified Couette flow at a lower Reynolds number, as given by the transformations in (2.30). Since the stratified bounding solutions can be identified with unstratified bounding solutions at lower Re, the associated mechanical energy dissipation rate in the bounding stratified flow is significantly less than that which is the bounding solution in the unstratified case at that particular Reynolds number.

There is a simple relationship between the long-time-averaged buoyancy flux and the mechanical energy dissipation rate for the bounding solutions. For asymptotically large Re, the energy input by the shear driving at the walls is split into three equal parts: buoyancy flux (essentially conversion into potential energy); dissipation by the horizontally averaged velocity profile (consisting of the combination of the background ϕ and the mean fluctuation $\overline{v_1}$); and dissipation by the meanless fluctuation $\hat{\boldsymbol{v}}$. This partition implies that, asymptotically, the flux Richardson number for the bounding solutions is $Ri_f \to 1/3$ as $Re \to \infty$. The fact that this asymptotic value differs from the result $Ri_f \to 1/2$ reported in CK01 for flows with piecewise linear background profiles is due to the conservative restriction in CK01 to flows with trivial meanless fluctuations $\hat{\boldsymbol{v}} = \boldsymbol{0}$ for the bounding solutions. Both situations have equipartition between the buoyancy flux and the dissipation owing to the horizontally averaged velocity profile. Since the full solution also has another non-trivial, and indeed equal, contribution from the meanless fluctuations, this inevitably reduces the flux Richardson number for the full solution to $1/3$ as $Re \to \infty$.

Furthermore, the numerical continuation method developed in PK03 and used here allows us to determine not only the asymptotic value of significant flow quantities, but also their values as a function of the controlling parameter Re. In particular, we are able to trace the variation of the flux Richardson number of the bounding solutions with Reynolds number. We show that typically observed values $Ri_f \sim 0.15{-}0.25$ occur for moderate Reynolds numbers $Re \sim 1000$, perhaps suggesting that the conventional parameterizations are appropriate only for flows with smaller Re, and may indeed by specific to the classical flows that have been considered (as discussed in the reviews of Fernando 1991; Peltier & Caulfield 2003). Since the flux Richardson number is derived directly from the bounding solutions, there is once again no dependence on overall stratification.

However, we certainly need to proceed with caution in such extrapolations for (at least) four important reasons. First, there is no reason to suppose that real flows actually do maximize buoyancy flux. Secondly, it is not at all clear that any results we identify from this specialized Couette flow can (or should) carry over into generic statements about stratified shear flows. In particular, the flow structure is clearly dominated by the moving boundaries, which are not a normal characteristic of geophysical turbulent flows. The properties of this model problem do need to be studied in detail numerically and experimentally to validate its use as a model problem. Thirdly, it is not clear that the bound is 'realizable', or attained by flows that actually satisfy the Navier–Stokes equations. Owing to the relationship between the fluctuation $\boldsymbol{v}$ and the actual fluid velocity $\boldsymbol{u}$, we actually optimize over a class that is a superset of the solutions to the true governing equations (2.1)–(2.3). As is well-known for the unstratified Couette flow and mentioned above (see PK03 for a fuller discussion), the mean flow distributions that are determined by generating an upper bound for the mechanical energy dissipation do not, in point of fact, correspond to experimentally observed flows, in particular because of the continued presence of

non-zero shear in the interior of the flow to asymptotically large Reynolds numbers. This structure (see figure 2) also persists in our stratified flow, thus calling into question whether the flows calculated here could actually be sustained in a real fluid. Finally, even if all these other problems are addressed, it is important to remember that our calculation has only generated a rigorous upper bound for the buoyancy flux. It is unclear how meaningful the associated value of the flux Richardson number for such solutions is, as the particular value of the mechanical energy dissipation rate for these optimizing solutions is not constrained in an obvious way, and indeed is substantially less than the possible upper bound for the dissipation itself. Drawing any strong conclusions about the properties of Ri_f at this time is therefore inappropriate.

Work is ongoing to address all of these concerns, in particular by directly simulating this flow at a range of Reynolds numbers. The bounding calculations presented in this paper have now given us a rigorous framework with which to compare the results of numerical simulation. Such comparisons will hopefully shed further light on the important problem of parameterization of stratified mixing.

We would like to thank Richard Kerswell, Charlie Doering and Peter Constantin for very many useful discussions on a wide range of issues raised in this paper. C. P. C. would also like to acknowledge the hospitality of the GFD summer study program in general, (and Dr Claudia Cenedese in particular) at the Woods Hole Oceanographic Institution during the summer of 2002, where this research problem was originally formulated. C. P. C. and W. T. gratefully acknowledge the support of NSF grant no. ATM-0222104, as part of the Research Collaborations between the Mathematical Sciences and the Geosciences (CMG) program. S. C. P. gratefully acknowledges the support of the EPSRC.

REFERENCES

Boyd, J. P. 2001 *Chebyshev and Fourier Spectral Methods,* 2nd Edn. Dover.

Busse, F. H. 1968 On the mean field problem of thermal convection. *Tech. Rep.* 8. Max-Planck-Institut für Physik und Astrophysik.

Busse, F. H. 1969*a* Bounds on the transport of mass and momentum by turbulent flow. *Z. angew. Math. Phys.* **20**, 1–14.

Busse, F. H. 1969*b* On Howard's upper bound for heat transport by turbulent convection. *J. Fluid Mech.* **37**, 457–477.

Busse, F. H. 1970 Bounds for turbulent shear flow. *J. Fluid Mech.* **41**, 219–240.

Busse, F. H. 1978 The optimum theory of turbulence. *Adv. Appl. Mech.* **18**, 77–121.

Caulfield, C. P. & Kerswell, R. R. 2001 Maximal mixing rate in turbulent stably stratified Couette flow. *Phys. Fluids* **13**, 894–900 (herein referred to as CK01).

Caulfield, C. P. & Peltier, W. R. 2000 The anatomy of the mixing transition in homogeneous and stratified free shear layers. *J. Fluid Mech.* **413**, 1–47.

Constantin, P. & Doering, C. R. 1995 Variational bounds on energy dissipation in incompressible flows: II. Channel flow. *Phys. Rev.* E **51**, 3192–3198.

Doering, C. R. & Constantin, P. 1992 Energy dissipation in shear driven turbulence. *Phys. Rev. Lett.* **69**, 1648–1651.

Doering, C. R. & Constantin, P. 1994 Variational bounds on energy dissipation in incompressible flows: shear flow. *Phys. Rev.* E **49**, 4087–4099.

Doering, C. R. & Constantin, P. 1996 Variational bounds on energy dissipation in incompressible flows: III. Convection. *Phys. Rev.* E **53**, 5957–5981.

Fernando, H. J. S. 1991 Turbulent mixing in stratified fluids. *Annu. Rev. Fluid Mech.* **23**, 455–493.

Gargett, A. E. & Moum, J. N. 1995 Mixing efficiencies in turbulent tidal fronts: results from direct and indirect measurements of density flux. *J. Phys. Oceanogr.* **25**, 2583–2608.

Gebhardt, T., Grossmann, S., Holthaus, M. & Löhden, M. 1995 Rigorous bound on the plane-shear-flow dissipation rate. *Phys. Rev.* E **51**, 360–365.

Hopf, E. 1941 Ein allgemeiner endlichkeitssatz der hydrodynamik. *Math. Annln* **117**, 764–775.

Howard, L. N. 1963 Heat transport by turbulent convection. *J. Fluid Mech.* **17**, 405–432.

Howard, L. N. 1972 Bounds on flow quantities. *Annu. Rev. Fluid Mech.* **4**, 473–494.

Howard, L. N. 1990 Limits on the transport of heat and momentum by turbulent convection with large scale flow. *Stud. Appl. Maths* **83**, 273–285.

Joseph, D. D. 1976 *Stability of Fluid Motions I*. Springer.

Kerswell, R. R. 1997 Variational bounds on shear-driven turbulence and turbulent Boussinesq convection. *Physica* D **100**, 355–376.

Kerswell, R. R. 1998 Unification of variational principles for turbulent shear flows: the background method of Doering–Constantin and the mean-fluctuation formulation of Howard–Busse. *Physica* D **121**, 175–192.

Kerswell, R. R. 2001 New results in the variational approach to turbulent Boussinesq convection. *Phys. Fluids* **13**, 192–209.

Linden, P. F. 1979 Mixing in stratified fluids. *Geophys. Astrophys. Fluid Dyn.* **13**, 2–23.

Malkus, W. V. R. 1954 The heat transport and spectrum of thermal turbulence. *Proc. R. Soc.* **225**, 196–212.

Malkus, W. V. R. 1956 Outline of a theory of turbulent shear flow. *J. Fluid Mech.* **1**, 521–539.

Monin, A. S. & Yaglom, A. M. 1971 *Statistical Fluid Mechanics: Mechanics of Turbulence*, vol. 1. MIT Press.

Moum, J. N. 1996 Efficiency of mixing in the main thermocline. *J. Geophys. Res.* C **5**, 12 057–12 069.

Nicodemus, R., Grossmann, S. & Holthaus, M. 1997*a* Improved variational principle for bounds on energy dissipation in turbulent shear flow. *Physica* D **101**, 178–190.

Nicodemus, R., Grossmann, S. & Holthaus, M. 1997*b* Variational bound on energy dissipation in plane Couette flow. *Phys. Rev.* E **56**, 6774–6786.

Nicodemus, R., Grossmann, S. & Holthaus, M. 1998*a* The background flow method. Part 1. Constructive approach to bounds on energy dissipation. *J. Fluid Mech.* **363**, 281–300.

Nicodemus, R., Grossmann, S. & Holthaus, M. 1998*b* The background flow method. Part 2. Asymptotic theory of dissipation bounds. *J. Fluid Mech.* **363**, 301–323.

Osborn, T. R. 1980 Estimates of the local-rate of vertical diffusion from dissipation measurements. *J. Phys. Oceanogr.* **10**, 83–89.

Pardyjak, E. R., Monti, P. & Fernando, H. J. S. 2002 Flux Richardson number measurements in stable atmospheric shear flows. *J. Fluid Mech.* **459**, 307–316.

Plasting, S. C. & Kerswell, R. R. 2003 Improved upper bound on the energy dissipation rate in plane Couette flow: the full solution to Busse's problem and the Constantin–Doering–Hopf problem with one-dimensional background field. *J. Fluid Mech.* **477**, 363–379 (herein referred to as PK03).

Peltier, W. R. & Caulfield, C. P. 2003 Mixing efficiency in stratified shear flows. *Annu. Rev. Fluid Mech.* **35**, 135–167.

Rheinboldt, W. C. & Burkhardt, J. V. 1983*a* ALGORITHM 596 a program for a locally parameterized continuation process. *ACM Trans. Math. Software* **9**, 236–241.

Rheinboldt, W. C. & Burkhardt, J. V. 1983*b* A locally parameterized continuation process. *ACM Trans. Math. Software* **9**, 215–235.

Ruddick, B., Walsh, D. & Oakey, N. 1997 Variations in apparent mixing efficiency in the North Atlantic central water. *J. Phys. Oceanogr.* **27**, 2589–2605.

Smyth, W. D., Moum, J. N. & Caldwell, D. R. 2001 The efficiency of mixing in turbulent patches: inferences from direct simulations and microstructure observations. *J. Phys. Oceanogr.* **31**, 1969–1992.

Strang, E. J. & Fernando, H. J. S. 2001 Entrainment and mixing in stratified shear flows. *J. Fluid Mech.* **428**, 349–386.

Townsend, A. A. 1958 The effects of radiative transfer on turbulent flow in a stratified fluid. *J. Fluid Mech.* **4**, 361–375.

Turner, J. S. 1973 *Buoyancy Effects in Fluids*. Cambridge University Press.